A closed-loop model for the coordination of gaze control and decision-making

Demetrio Ferro[1], Tianming Yang[2], Rubén Moreno-Bote[1]

[1]Center for Brain and Cognition, Dept. of Information and Comm. Technologies, Universitat Pompeu Fabra, 08002, Barcelona, Spain; [2]Institute of Neuroscience, Chinese Academy of Sciences, 200031, Shanghai, China

Abstract

The study of **neural circuitry** in **visually-guided decision-making** has inspired models of *decision formation*. However, the role of **gaze** in enabling *focal sampling* and shifts to alternative options remains unclear. We propose a **closed-loop model** integrating *gaze signals* with **decision dynamics** for optimized visual sampling. *Visual input* activates **decision populations**, competing via *mutual inhibition*. Their output drives **gaze populations**, producing *visual shifts* that feed back into the **decision process**. Simulations on a **two-alternative bundle task** show that **gaze** and **choice** behavior align in terms of *accuracy* and *gaze shift frequency*. The model predicts, for example, that *fewer gaze shifts* correlate with *shorter reaction times*, and that shifts may coincide with changes in **neural value encoding**. It can also be extended to **sequential choices** or contexts with **distractors**, where gaze is an important value reactivation correlate [1].

Simulation Outline
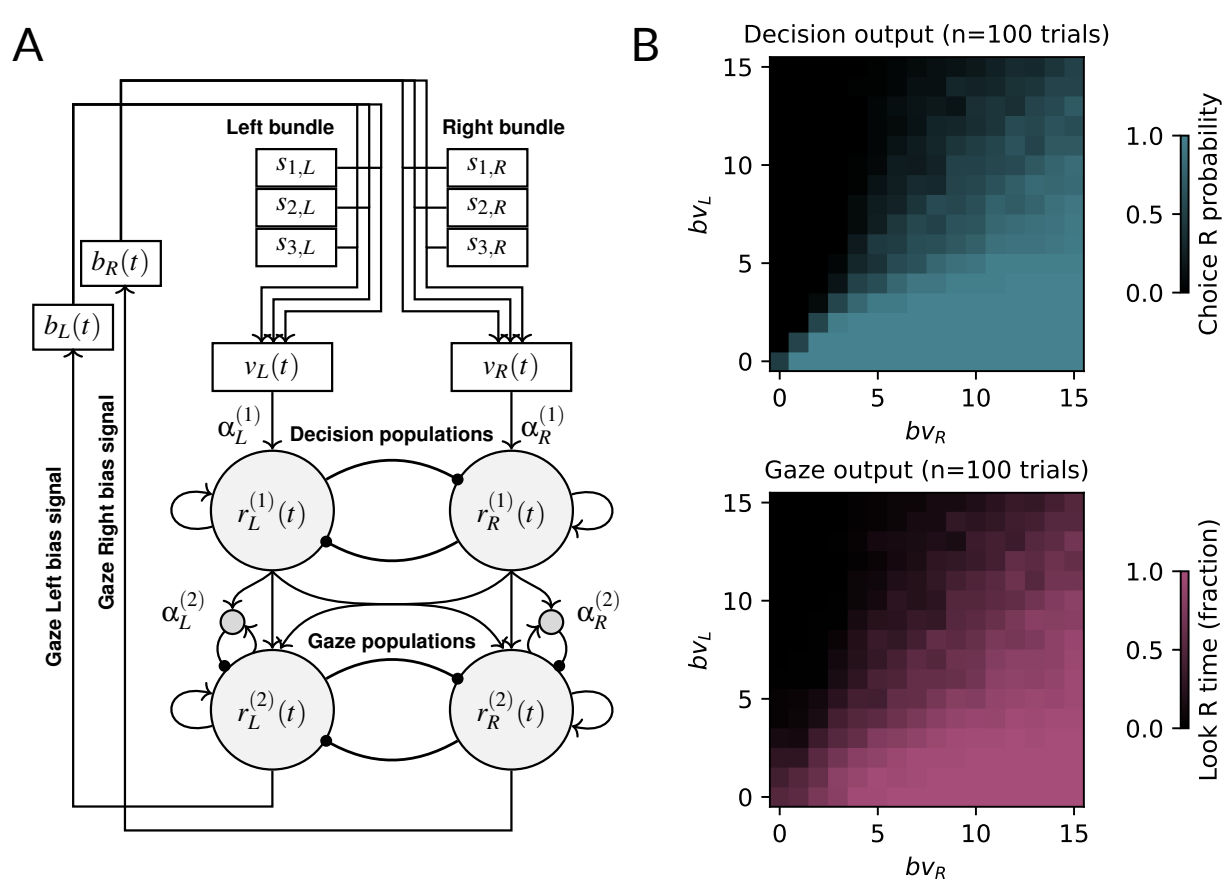
Figure 1. Model diagram and simulation results. A. Model diagram outline. **B.** Probability of choosing right (top) and fraction of time directing gaze to right side (bottom) for pairs of bundle values (bv_R, bv_L). Parameters used: $dt = 0.1$ ms; $\tau^{(1)} = 100$ ms; $\tau^{(2)} = 30$ ms; $w_{LL}^{(1)}, w_{RR}^{(1)} = 0.05$; $w_{LR}^{(1)}, w_{RL}^{(1)} = -1$; $w_{LL}^{(2)}, w_{RR}^{(2)} = 0.5$; $w_{LR}^{(2)}, w_{RL}^{(2)} = -2$; $\alpha^{(1)} = 1$; $\alpha^{(2)} = 0.1$; $\sigma_{(1)} = 5$; $\sigma_{(2)} = 0.08$; $\tau_\xi = 1000$ ms; $b_0 = 0$; $b_1 = 1$; $n = 100$ runs.

Methods

The interaction between decision formation and gaze direction is modeled by hypothesizing mutual inhibition between the respective (1, decision; 2, gaze) population pairs (each containing L, left or R, right units). The bundle shapes ($s_{k,L}, s_{k,R}, k = 1, 2, 3$) are visually sampled by multiplication to gaze bias signals ($b_L(t), b_R(t)$). The left or right bundle sampling is fed to the respective decision populations through scaling factors ($\alpha_L^{(1)}, \alpha_R^{(1)}$), implementing choice formation. The output of decision populations is combined through scaling factors ($\alpha_L^{(2)}, \alpha_R^{(2)}$) to gaze populations implementing attractor networks with perceptual bistability, allowing alternations induced by noise fluctuations [3]. The gaze bias signals ($b_L(t), b_R(t)$) are fed back to the visual sampling.

The two L/R firing rates pairs ($r_L^{(i)}(t), r_R^{(i)}(t), i = 1, 2$) are modeled as

$$\tau_L^{(i)} \frac{dr_L^{(i)}}{dt} = -r_L^{(i)}(t) + f\left(w_{RL}^{(i)} r_R^{(i)}(t) + w_{LL}^{(i)} r_L^{(i)}(t) + I_L^{(i)}(t) + \xi_L^{(i)}(t)\right),$$
$$\tau_R^{(i)} \frac{dr_R^{(i)}}{dt} = -r_R^{(i)}(t) + f\left(w_{LR}^{(i)} r_L^{(i)}(t) + w_{RR}^{(i)} r_R^{(i)}(t) + I_R^{(i)}(t) + \xi_R^{(i)}(t)\right) \quad (1)$$

$$v_L(t) = b_L(t) \sum_{k=1}^{3} s_{k,L}, \quad I_L^{(1)} = \alpha_L^{(1)} v_L(t)$$
$$v_R(t) = b_R(t) \sum_{k=1}^{3} s_{k,R}, \quad I_R^{(1)} = \alpha_R^{(1)} v_R(t) \quad (2)$$

$$g_L(t) = \alpha_L^{(2)} r_L^{(1)}(t), \quad I_L^{(2)}(t) = g_L(t) - (g_L(t) + g_R(t)) r_L^{(2)}(t)$$
$$g_R(t) = \alpha_R^{(2)} r_R^{(1)}(t), \quad I_R^{(2)}(t) = g_R(t) - (g_R(t) + g_L(t)) r_R^{(2)}(t) \quad (3)$$

$\xi_L^{(1)}(t), \xi_R^{(1)}(t) \sim \mathcal{N}(0, \sigma_{(1)}^2)$, while $\xi_L^{(2)}(t), \xi_R^{(2)}(t)$ are Ornstein-Uhlenbeck processes

$$\frac{d\xi^{(2)}}{dt} = -\frac{\xi^{(2)}(t)}{\tau_\xi} + \sigma_{(2)}\sqrt{2/\tau_\xi} z(t), \quad z(t) \sim \mathcal{N}\left(0, \sigma_{(2)}^2\right), \quad (4)$$

and steady-state distribution $\sim \mathcal{N}(0, \sigma_{(2)}^2/(2\tau_\xi))$.

We used **ReLU** for decision populations, modeling thresholded accumulation, and **tanh** for gaze populations, following general practice respectively from evidence accumulation and bistable switching neural dynamic models. We define feedback gaze bias:

$$b_L(t) = b_0 + b_1 \frac{|r_L^{(2)}(t)|}{|r_L^{(2)}(t)| + |r_R^{(2)}(t)|}, \quad b_R(t) = b_0 + b_1 \frac{|r_R^{(2)}(t)|}{|r_L^{(2)}(t)| + |r_R^{(2)}(t)|}. \quad (5)$$

Results
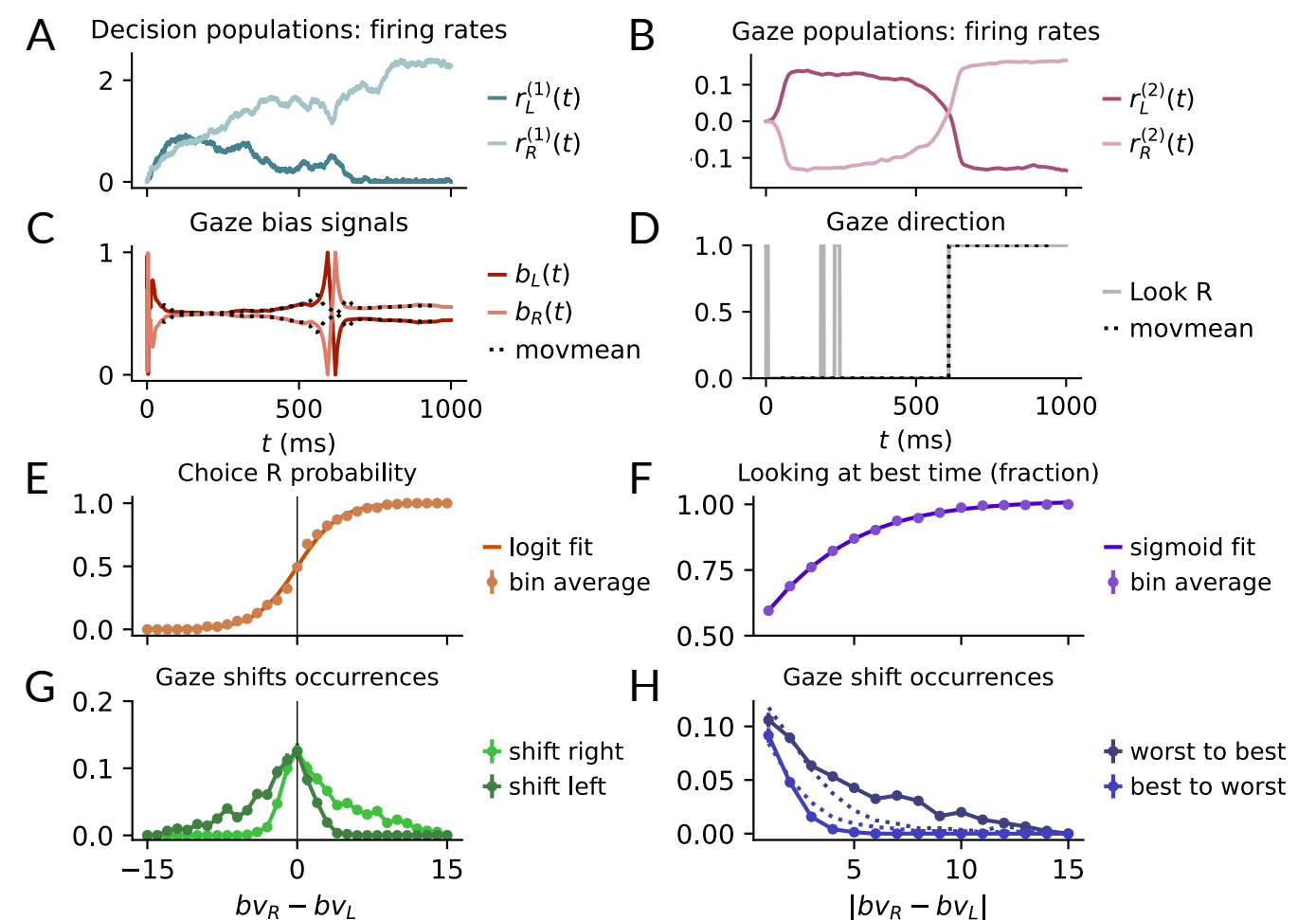
Figure 2. Firing rates and predicted behavioral outputs. Firing rate of the L/R Decision populations (**A.**) and L/R Gaze populations (**B.**) for a sample configuration ($bv_L = 4, bv_R = 5$). Gaze bias signals (**C.**) and Gaze direction (**D.**) for the same bv_L, bv_R configuration, including moving mean filtered versions (dotted, movmean). Predicted psychometrics for different bundle value differences: probability of right bundle choice and logistic fit (**E.**), fraction of time looking at best option and sigmoid function fit (**F.**), average occurrence of gaze shifts between the two bundles sides (**G.**) and of gaze shifts towards best/worst option (**H.**), with dotted lines showing comparison with gaze shifts from empirical data by Huang et al. [2].

Further details and future directions

The two-alternative bundles decision-making task. The two-alternative bundles task [2] consists in the simultaneous presentation of two visual bundles, each containing 3 items disposed vertically on the left or the right of the screen. The items are associated with rewards whose value ranges from 0 to 5. The value of bundles is given by the sum of item values. Decisions are reported via gaze fixation to the target bundle for at least 0.4 s. Choices are correct if the highest value bundle is selected, rewarded with liquid of size proportional to the bundle value. Incorrect choices incur a 3 s time-out penalty.

Gaze and Decision output. The simulated choice is sampled at $T = 1$ s: choose R if $r_R^{(1)}(T) > r_L^{(1)}(T)$, choose L otherwise. This does not preclude making more detailed assumptions about choice deliberation that may occur earlier, eventually indicated via gaze fixation. We apply a moving mean filter (movmean) on gaze bias signals using boxcar time windows with duration 100 ms and shifted at each 10 ms offsets. The gaze direction output is determined as: Look R if movmean($b_R(t)$) >movmean($b_L(t)$), Look L otherwise.

Choice probability and looking times. The fraction of choices for the right bundle (Fig. 2E) is computed in discrete bins of bundle value difference, and overlaid to the logistic fit of trial-based data, modeling $P(ch = R) = 1/(1 + e^{-\beta_0 - \beta_1(bv_R - bv_L)})$. The average fraction of time looking at best bundle (Fig. 2F is binned by absolute bundle value difference. Trial-based data are fit to $F_{best} = a_0 + a_1/(1 + e^{-\beta_0' - \beta_1'|bv_R - bv_L|})$. Gaze shifts (Fig. 2G-H) are defined as discrete-time discontinuities in Look L / Look R, computed in 10 ms bins.

Future directions. The results shown here qualitatively align with behavioral patterns reported by Huang et al. (2024), though direct overlays are shown only for gaze shifts (Fig. 1H) due to partial data availability. At the current stage, other panels could are qualitatively compared against the same dataset. Beyond this, the model supports testable predictions about gaze–choice interactions, e.g., whether **fewer gaze shifts** lead to **shorter reaction times**, or if gaze **shifts** coincide with neural encoding **alternations**, or bidirectional effects such as **decision-related** gaze bias[1]. The model can be extended to explore gaze–decision dynamics across more complex paradigms and neural structures such as LIP or FEF involved in **oculomotor planning** and **value encoding**.

References

[1] Demetrio Ferro, Tyler Cash-Padgett, Maya Zhe Wang, Benjamin Y Hayden, and Rubén Moreno-Bote. Gaze-centered gating, reactivation, and reevaluation of economic value in orbitofrontal cortex. *Nature Communications*, 15(1):6163, 2024.

[2] Yuxi Huang, Rui Zhu, Ruichang Sun, Wenyi Zhang, Chi Ren, Zhengtuo Zhao, and Tianming Yang. Value computation of offer bundles in prefrontal circuits during economic decision-making. In *The 17th Annual Meeting of Chinese Neuroscience Society*, 2024.

[3] Rubén Moreno-Bote, John Rinzel, and Nava Rubin. Noise-induced alternations in an attractor network model of perceptual bistability. *Journal of neurophysiology*, 98(3):1125–1139, 2007.